

Research Article

**Use of N-(4-aminophenyl)piperidine Derivatization to Improve Organic Acid Detection
with Supercritical Fluid Chromatography-Mass Spectrometry**

Yih Ling Saw¹, John R. Boughton¹, Faith L. Wroniuk¹, Mahmoud Elhusseiny Mostafa²,
Peter J. Pellegrinelli¹, Samantha A. Calvez¹, Alexander S. Kaplitz¹, Lark J. Perez¹,
James L. Edwards², James P. Grinias^{1,*}

¹Department of Chemistry & Biochemistry, Rowan University, Glassboro, NJ USA

²Department of Chemistry, Saint Louis University, St. Louis, MO USA

*Corresponding Author: J.P.G. (grinias@rowan.edu)

Keywords: Supercritical Fluid Chromatography, SFC-MS, Chemical Derivatization, Organic Acids

Abstract

The analysis of organic acids in complex mixtures by LC-MS can often prove challenging, especially due to the poor sensitivity of negative ionization mode required for detection of these compounds in their native (i.e. underivatized, or untagged) form. These compounds have also been difficult to measure using SFC-MS, a technique of growing importance for metabolomic analysis, with similar limitations based on negative ionization. In this report, the use of a high proton affinity N-(4-aminophenyl)piperidine derivatization tag is explored for the improvement of organic acid detection by SFC-MS. Four organic acids (lactic, succinic, malic, and citric acids) with varying numbers of carboxylate groups were derivatized with N-(4-aminophenyl)piperidine to achieve detection limits down to 0.5 ppb, with overall improvements in detection limit ranging from 25- to-2100-fold. The effect of the derivatization group on sensitivity, which increased by at least 200-fold for compounds that were detectable in their native form, and mass spectrometric detection are also described. Preliminary investigations into the separation of these derivatized compounds identified multiple stationary phases that could be used for complete separation of all four compounds by SFC. This derivatization technique provides an improved approach for the analysis of organic acids by SFC-MS, especially for those that are undetectable in their native form.

1. Introduction

Monitoring small molecule metabolites plays an important role in understanding complex biological systems and has been used extensively in the areas of clinical diagnostics, drug development, toxicology, and pharmacology [1]. One important class of metabolites is organic acids, which are involved in various metabolic pathways, including the Cori and Krebs cycles [2]. Because of their involvement in these processes, the analysis of organic acids can provide crucial insight into a variety of important cellular mechanisms [3–5]. However, there are several challenges to effectively characterizing these compounds using LC-MS. Because of their high polarity, native (i.e. underivatized, or untagged) organic acids have been separated using HILIC [6,7], but this approach can require lengthy column re-equilibration steps between injections [8,9]. Ion-exchange chromatography has also been used for the separation of organic acids, although challenges exist when coupling this technique to MS [10]. A recent review detailed such methods used for the analysis of these compounds in biological samples by liquid chromatography [11]. Because of their carboxylic acid functional groups, these compounds are typically detected by ESI-MS in negative mode, which generally suffers from lower signal intensity than positive mode [11–13]. These challenges provide motivation for the development of new analytical techniques for the analysis of organic acids.

Supercritical fluid chromatography (SFC) coupled to MS is increasingly being adopted for metabolomic applications because of its compatibility with a broad range of both hydrophilic and hydrophobic compounds [1,14]. Additionally, its faster re-equilibration time provides for higher analytical throughput than HILIC [15]. SFC-MS has specifically been used for the analysis of organic acids in multiple reports [14–16]. However, negative ionization mode is still typically employed for ESI in these methods, which can decrease sensitivity [17]. To address this issue,

chemical derivatization can be employed to enhance the proton affinity of organic acid metabolites and permit detection in positive mode ESI [18]. Recently, the use of N-(4-aminophenyl)piperidine to derivatize carboxyl groups in organic acids increased sensitivity in LC-MS analysis up to 20-fold relative to the native compound [19]. In this study, such an approach was adapted for use in SFC-MS, with a focus on the identification of method parameters that best improved analyte signal. The separation of these compounds was also examined by exploring compound retention on three different stationary phases.

2. Materials and Methods

2.1. Reagents

L-lactic acid, succinic acid, D-malic acid, citric acid, hexafluorophosphate azabenzotriazole tetramethyl uronium (HATU), dimethyl sulfoxide (DMSO), ammonium acetate, and N-(4-aminophenyl)piperidine were purchased from Sigma Aldrich (St. Louis, MO). Methanol (LC-MS grade), dimethylformamide (DMF), dichloromethane (DCM), N,N-diisopropylethylamine (DIPEA), sodium sulfate, formic acid, and acetic acid were purchased from VWR (Radnor, PA). Reagent grade ethyl acetate (EtOAc), hexanes, sodium bicarbonate, and sodium chloride were purchased from Greenfield Global (Brookfield, CT). HiPerSolv Chromanorm ethanol (90%, denatured with 5% isopropanol and 5% methanol) was also acquired from VWR. High-purity (instrument grade 4.0) carbon dioxide was purchased from Praxair (Danbury, CT). Buffered mobile phase modifiers were 10 mM ammonium acetate in methanol (or ethanol when noted, both adjusted to pH 5.5 with acetic acid) and 0.1% formic acid (v/v) in methanol.

2.2 Derivatization and Preparation of Organic Acid Samples

The general synthetic route is shown in **Figure 1**. Briefly, in a 20 mL screw cap vial equipped with a magnetic stir bar, each organic acid (0.142 mmol, mass variable depending on structure, 1.0 molar eq.) was dissolved in DMF (1.4 mL, 0.1 M) and treated with DIPEA (3.0 molar eq. per carboxylic acid) and N-(4-aminophenyl)piperidine (1.0 molar eq. per carboxylic acid as a 0.5 M stock solution in DMF). This mixture was then treated with HATU (1.2 molar eq. per carboxylic acid) in a single portion. The resulting mixture was allowed to react at ambient temperature for 2 h and was transferred to a separatory funnel containing 30 mL DCM and 30 mL saturated aqueous NaHCO₃. The layers were separated and the aqueous layer was extracted with DCM (2 x 20 mL). The combined organic layers were washed with saturated aqueous NaCl solution, dried over Na₂SO₄, and concentrated *in vacuo*. The resulting crude mixture was purified to generate more pure samples for further investigation by flash chromatography (Biotage Isolera, 60 µm silica, 25 g column) using a gradient of 20% EtOAc/hexanes to 100% EtOAc. Further details on the specific synthesis for each compound and further characterization details can be found in the *Supplementary Information*. Following derivatization and purification, individual compounds were dried by vacuum and reconstituted in methanol (except for citrate, which was reconstituted in DMSO to improve solubility) to a stock concentration of 5 mg/mL. Native, untagged organic acids were also prepared in stock solutions of 5 mg/mL. Further dilutions to the working concentrations were all made with methanol. All samples were filtered with a 0.2 µm syringe filter prior to injection.

2.3 Instrumentation, Columns, and Analysis

All experiments were performed using a Nexera UC SFC-MS system (Shimadzu, Kyoto, Japan) consisting of CO₂ and modifier solvent delivery pumps, autosampler, column oven, photodiode array (PDA) detector, backpressure regulator (BPR), make-up flow pump, and LCMS-2020 single quadrupole mass spectrometer. The column oven and BPR were set at 40 °C and 130 bar, respectively. Three stationary phases were used in this study, all in 3.0 x 150 mm format columns: HALO Penta-HILIC 5 µm 90 Å superficially porous particles (Advanced Materials Technology, Wilmington, DE), Chirex 3014 5 µm 120 Å fully porous particles (Phenomenex, Torrance, CA), and Luna Omega Sugar 3 µm 100 Å fully porous particles (Phenomenex, Torrance, CA). For analyte signal characterization, the Penta-HILIC column was equilibrated for 15 min at the operating flow rate of 1.5 mL/min with a mobile phase (isocratic elution conditions) consisting of 85% CO₂ and 15% methanol (with 10 mM ammonium acetate, pH 5.5). Injection volume was set at 2 µL and injections were performed in triplicate. When make-up flow was employed (0.15 mL/min flow rate), the additional eluent was added into the flow stream before the BPR. Parameters for the LCMS-2020 used for MS detection for both native and derivatized organic acids are available in **Table S1**. Limit of detection (LOD), limit of quantification (LOQ) and sensitivity for each compound were evaluated via serial dilution of the native and derivatized organic acids over a range of 10 ng/mL (ppb) – 300 µg/mL (ppm). The LOD and LOQ were determined using the signal-to-noise ratio (S/N) at the lowest concentration measured to calculate the concentrations giving S/N ratios of 3 and 10, respectively, per previous published methodology used for similar analytes [20]. The signal was calculated as the max peak intensity above the baseline, and noise was the standard deviation of the baseline across 1 min near the peak. Data were processed in the instrument LabSolutions software (Shimadzu, Kyoto, Japan) and Microsoft

Excel (Redmond, WA). Figures were generated using Igor Pro 6.0 (Wavemetrics, Lake Oswego, OR).

3. Results and Discussion

3.1 Effect of Derivatization on Organic Acid Detection

Organic acids are a difficult class of metabolites to characterize by LC-MS or SFC-MS due to their high polarity and chemical functionality that typically require negative ionization mode for detection. In this study, we focused on the detection of four common organic acids (lactic, succinic, malic, and citric) and compared signal intensity between native compounds and those that had been derivatized with a N-(4-aminophenyl)piperidine group. As shown in **Figure 2**, the peak signal for the two native organic acids that were detectable using SFC-MS, lactic acid and succinic acid, was less than 30,000 counts (signal-to-noise ratios of 9 and 88, respectively). Following derivatization, the peak signal was enhanced over 100-fold as the tag increased proton affinity and allowed for higher intensity positive ionization. Peak signal calibration curves for native and derivatized compounds (**Figure 3**) demonstrate an average 430-fold increase in sensitivity for the compounds that were detectable in their native form. Calculated LODs, LOQs, and sensitivities for both compound sets based on these curves are shown in Table 1. The improvement in LOD varied from 25-fold for succinic acid to 2100-fold for lactic acid, with detection becoming possible for malic acid and citric acid post-derivatization. This is similar to previous observations in LC-MS for the derivatized compounds and demonstrates that the benefits of the N-(4-aminophenyl)piperidine tag can be extended to SFC-MS [19]. Although studies using SFC-MS that included compounds from this set did not include detection limits [14,15], some comparisons can be made to recent studies using LC-MS with negative ionization mode. For the

compounds measured here, reported LOD ranges are 0.1 - 700 ppb, 0.2 - 200 ppb, 1.1 - 100 ppb, and 27 - 700 ppb for native lactate, succinate, malate, and citrate, respectively [7][21–24]. The values reported in Table 1 correspond favorably to these ranges, although the comparisons are not direct as some studies may have higher values due to matrix effects and all the cited LC studies utilized triple quadrupole MS systems while this report utilized a single quadrupole MS. Further, as shown in **Figure 2**, peak shape improvement was also observed following derivatization. Extra column band broadening is a known challenge in SFC [25,26], and here the extra-column volume of \sim 110 μ L was nearly 20% of the column volume. It is possible that with further improvements to reduce system-based band broadening and increase signal-to-noise ratios, along with more sensitive MS techniques, LODs could be even further improved.

The data described above were obtained using selected ion monitoring (SIM) mode targeting the maximum peak identified in full scan mode (full scans shown in **Figure S1** and primary mass-to-charge ratios listed in **Table S2**). Even if multiple ionization sites were available in the native organic acids, the highest intensity signal was observed for the molecular ion $[M-H]^-$ in negative mode. For the derivatized compounds, the base peak varied with the number of tags, showing highest intensity for the molecular ion $[M+H]^+$ for the singly tagged analyte, $[M+K]^+$ for the doubly tagged analytes, and $[M+2H]^{2+}$ for the triply tagged analyte. Potassium ions can form metal ion clusters with alcohol modifiers to produce potassium adducts ($[M+K]^+$), which may result in ion suppression in SFC-MS [1,27]. Because the repeatability of such adduct peaks can be lower than the protonated peaks, they are less frequently used for quantitation [28]. Despite the spread of signal across multiple charge states and the presence of potassium adducts, the overall larger increase in signal intensity still permits a significant increase in sensitivity and improvements to detection limits for the derivatized compounds that could be useful in future

metabolomic experiments using SFC-MS. In addition, multiple groups have reported difficulties measuring native organic acids using SFC-MS [14,15], which was also experienced here with malic and citric acids. With N-(4-aminophenyl)piperidine derivatization, the measurement of these compounds was achieved.

3.2 Effects of Modifier Additives and Make-Up Flow on Signal Intensity

Two key aspects in SFC-MS method development are the use of additives in the mobile phase modifier and the amount of make-up flow needed to ensure that the eluent stream is effectively delivered to the MS inlet after the backpressure regulator. For the analysis of derivatized organic acids, buffer additives can also play a crucial role in the ionization state of the compounds, affecting both their separation and detection [29,30]. In this study, two common additives in SFC-MS, ammonium acetate (10 mM, pH 5.5) and formic acid (0.1% v/v), were investigated for their effect on a dicarboxylic acid (succinic acid) along with pure methanol as the primary organic modifier. For derivatized succinic acid, the use of ammonium acetate provided the highest signal intensity (**Figure 4**). With 0.1% formic acid, the doubly charged ion was more intense than the singly charged ion, but the signal of both charge states was slightly decreased relative to the other modifier conditions used. The effects of ammonium acetate were similar to previously observed effects on peak shape and signal intensity with this additive [31]. Because of the higher signal, preferential ionization to a single charge state, and improved peak shape, ammonium acetate was selected as the preferred additive to the methanol organic modifier for the derivatized compounds. One exception to this trend was citric acid, which had slightly higher intensity for the doubly charged peak ($[M+2H]^{2+}$) than the singly charged peak ($[M+H]^+$) (**Figure**

S1). In general, the overall signal enhancement across the full range of compounds suggests ammonium acetate as the preferred additive.

Make-up flow in SFC-MS is typically used to promote ionization of analytes and better transport of the eluent stream following the backpressure regulator, where expansion of the carbon dioxide can begin to occur [32,33]. Here, the effect of an additional 0.15 mL/min make-up flow (10% of 1.5 mL/min total mobile phase flow rate) on derivatized succinic acid was tested to see if similar improvement was observed. As shown in **Figure 5**, the use of make-up flow did not increase the overall signal intensity, and decreased the signal when ammonium acetate was present in the make-up flow solvent. However, when the make-up flow included the ammonium acetate additive, the relative intensity of the singly charged ionization state to the doubly charged state was higher (**Figure S2**). Based on previous literature study, the loss of compressibility of CO₂ post-BPR may enhance precipitation of analytes and loss of chromatographic integrity, hence posing a significant challenge towards detection of the analytes by SFC-MS [33]. For these derivatized compounds, the ability to effectively detect them by SFC-MS without make-up flow enables simpler operation of the technique by requiring one less mobile phase pump. For quantitative measurements, the use of make-up flow may improve signal stability over time, even for compounds that do not necessarily see differences in signal response [34]. However, the best approach to improve quantitative repeatability for these compounds may be to include stable isotope internal standards of the derivatized analytes for absolute quantitation [18].

3.3 Preliminary Column Screen for Separation of Derivatized Organic Acids

The primary focus of this study was the effect of N-(4-aminophenyl)piperidine derivatization on the MS signal intensity of organic acids under SFC elution conditions. However,

for eventual implementation in SFC-MS metabolomics, conditions for analyte separation by SFC will also be needed. To that end, three columns were screened for analyte separation using SFC-MS. Maintaining the 15% methanol modifier with 10 mM ammonium acetate additive, the separation of the four derivatized organic acids on these columns is shown in **Figure 6**. All three columns demonstrated the same order of elution based on the number of derivatization moieties. The highest resolution for the derivatized dicarboxylic acids (typical critical pair) was obtained with the Penta-HILIC column while the overall highest retention for compounds was observed using the Chirex 3014 column (which had previously been used for compounds with similar structural characteristics to the derivatized organic acids [35]). Separation was further investigated using the Penta-HILIC column, with retention expectedly decreasing with increasing modifier amount from 10% to 20% (**Figure S3**). As ethanol is a common alternative to methanol as a modifier for SFC separations [36], its use was also tested (**Figure S4**). Ethanol is a weaker modifier than methanol when using polar stationary phases in SFC, so the retention increased significantly with ethanol, especially for tagged citric acid. The ethanol modifier also resulted in lower SFC-MS signal intensity, likely due to an increase in gas-phase proton affinity compared to methanol [37], leading to methanol as the preferred organic solvent for the separation and detection of the derivatized organic acids.

4. Conclusions

The separation and detection of organic acids can be a challenging analytical task, with various issues occurring with HILIC, SFC, and MS detection. Here, a strategy employing N-(4-aminophenyl)piperidine of carboxylic acid groups in these molecules was demonstrated. The detection sensitivity of four commonly monitored compounds in this analyte class was increased

significantly over native forms, providing an improved technique for their measurement. Additionally, analytes that were not observed in native form (malic and citric acids) were easily measured by SFC-MS once derivatized. LOD values compared favorably to previous studies measuring the native compounds using LC-QqQ-MS. Further exploration of derivatized succinic acid identified ammonium acetate as an effective modifier additive and the capability to maintain analyte signal without SFC make-up flow, which is commonly used for SFC-MS methods. In the future, this derivatization strategy will be used for the analysis of these compounds using nanospray SFC techniques [38,39] to further enhance MS signal intensity. With these improvements, the method can be applied to a variety of biological samples, as has been demonstrated for other high proton affinity tags added to carboxylic acid groups [40].

Acknowledgements

The authors would like to thank Jason Anspach (Phenomenex) and Stephanie Schuster (Advanced Materials Technology) for generously providing the columns used in this study. This work was supported by funding from the Chemical Measurement and Imaging Program in the National Science Foundation Division of Chemistry to J.P.G. (CHE-1904454) and to J.L.E. (CHE-1904919).

Conflict of Interest Statement

The authors have declared no conflict of interest.

References

[1] van de Velde B, Guillarme D, Kohler I, Supercritical fluid chromatography – Mass spectrometry in metabolomics: Past, present, and future perspectives. *J. Chromatogr. B* 2020; **1161**: 122444. <https://doi.org/10.1016/j.jchromb.2020.122444>.

[2] Gowda GAN, Zhang S, Gu H, Asiago V, Shanaiah N, Raftery D, Metabolomics-based methods for early disease diagnostics. *Expert Rev. Mol. Diagn.* 2008; **8**: 617–633. <https://doi.org/10.1586/14737159.8.5.617>.

[3] Marunaka Y, The proposal of molecular mechanisms of weak organic acids intake-induced improvement of insulin resistance in diabetes mellitus via elevation of interstitial fluid pH. *Int. J. Mol. Sci.* 2018; **19**: 3244. <https://doi.org/10.3390/ijms19103244>.

[4] Goldberg I, Rokem JS, Pines O, Organic acids: Old metabolites, new themes. *J. Chem. Technol. Biotechnol.* 2006; **81**: 1601–1611. <https://doi.org/10.1002/jctb.1590>.

[5] Igamberdiev AU, Bykova N V., Role of organic acids in the integration of cellular redox metabolism and mediation of redox signalling in photosynthetic tissues of higher plants. *Free Radic. Biol. Med.* 2018; **122**: 74–85. <https://doi.org/10.1016/j.freeradbiomed.2018.01.016>.

[6] Tang DQ, Zou L, Yin XX, Ong CN, HILIC-MS for metabolomics: An attractive and complementary approach to RPLC-MS. *Mass Spectrom. Rev.* 2016; **35**: 574–600. <https://doi.org/10.1002/mas.21445>.

[7] Huang Y, Tian Y, Zhang Z, Peng C, A HILIC-MS/MS method for the simultaneous determination of seven organic acids in rat urine as biomarkers of exposure to realgar. *J. Chromatogr. B* 2012; **905**: 37–42. <https://doi.org/10.1016/j.jchromb.2012.07.038>.

[8] McCalley D V., A study of column equilibration time in hydrophilic interaction

chromatography. *J. Chromatogr. A* 2018; **1554**: 61–70.
<https://doi.org/10.1016/j.chroma.2018.04.016>.

[9] Kohler I, Verhoeven M, Haselberg R, Gargano AFG, Hydrophilic interaction chromatography – mass spectrometry for metabolomics and proteomics: state-of-the-art and current trends. *Microchem. J.* 2022; **175**: 106986.
<https://doi.org/10.1016/j.microc.2021.106986>.

[10] Ngere JB, Ebrahimi KH, Williams R, Pires E, Walsby-Tickle J, McCullagh JSO, Ion-Exchange Chromatography Coupled to Mass Spectrometry in Life Science, Environmental, and Medical Research. *Anal. Chem.* 2023; **95**: 152–166.
<https://doi.org/10.1021/acs.analchem.2c04298>.

[11] Fujiwara T, Inoue R, Ohtawa T, Tsunoda M, Liquid-Chromatographic Methods for Carboxylic Acids in Biological Samples. *Molecules* 2020; **25**: 4883.
<https://doi.org/10.3390/molecules25214883>.

[12] Cech NB, Enke CG, Practical implications of some recent studies in electrospray ionization fundamentals. *Mass Spectrom. Rev.* 2001; **20**: 362–387.
<https://doi.org/10.1002/mas.10008>.

[13] Rao W, Pan N, Tian X, Yang Z, High-Resolution Ambient MS Imaging of Negative Ions in Positive Ion Mode: Using Dicationic Reagents with the Single-Probe. *J. Am. Soc. Mass Spectrom.* 2016; **27**: 124–134. <https://doi.org/10.1007/s13361-015-1287-7>.

[14] Desfontaine V, Losacco GL, Gagnebin Y, Pezzatti J, Farrell WP, González-Ruiz V, Rudaz S, Veuthey JL, Guillarme D, Applicability of supercritical fluid chromatography – mass spectrometry to metabolomics. I – Optimization of separation conditions for the simultaneous analysis of hydrophilic and lipophilic substances. *J. Chromatogr. A* 2018;

1562: 96–107. <https://doi.org/10.1016/j.chroma.2018.05.055>.

[15] Sen A, Knappy C, Lewis MR, Plumb RS, Wilson ID, Nicholson JK, Smith NW, Analysis of polar urinary metabolites for metabolic phenotyping using supercritical fluid chromatography and mass spectrometry. *J. Chromatogr. A* 2016; **1449**: 141–155. <https://doi.org/10.1016/j.chroma.2016.04.040>.

[16] Herniman JM, Worsley PR, Greenhill R, Bader DL, John Langley G, Development of ultra-high-performance supercritical fluid chromatography-mass spectrometry assays to analyze potential biomarkers in sweat. *J. Sep. Sci.* 2022; **45**: 542–550. <https://doi.org/10.1002/jssc.202100261>.

[17] Cech NB, Enke CG, Electrospray and MALDI Mass Spectrometry: Fundamentals, Instrumentation, Practicalities, and Biological Applications: Second Edition. 2012; , pp. 49–73.

[18] Huang T, Armbruster MR, Coulton JB, Edwards JL, Chemical Tagging in Mass Spectrometry for Systems Biology. *Anal. Chem.* 2019; **91**: 109–125. <https://doi.org/10.1021/acs.analchem.8b04951>.

[19] Guan S, Armbruster MR, Huang T, Edwards JL, Bythell BJ, Isomeric Differentiation and Acidic Metabolite Identification by Piperidine-Based Tagging, LC-MS/MS, and Understanding of the Dissociation Chemistries. *Anal. Chem.* 2020; **92**: 9305–9311. <https://doi.org/10.1021/acs.analchem.0c01640>.

[20] Kloos D, Derkx RJE, Wijtmans M, Lingeman H, Mayboroda OA, Deelder AM, Niessen WMA, Giera M, Derivatization of the tricarboxylic acid cycle intermediates and analysis by online solid-phase extraction-liquid chromatography-mass spectrometry with positive-ion electrospray ionization. *J. Chromatogr. A* 2012; **1232**: 19–26.

<https://doi.org/10.1016/j.chroma.2011.07.095>.

- [21] Michopoulos F, Whalley N, Theodoridis G, Wilson ID, Dunkley TPJ, Critchlow SE, Targeted profiling of polar intracellular metabolites using ion-pair-high performance liquid chromatography and -ultra high performance liquid chromatography coupled to tandem mass spectrometry: Applications to serum, urine and tissue extracts. *J. Chromatogr. A* 2014; **1349**: 60–68. <https://doi.org/10.1016/j.chroma.2014.05.019>.
- [22] Buescher JM, Moco S, Sauer U, Zamboni N, Ultrahigh performance liquid chromatography-tandem mass spectrometry method for fast and robust quantification of anionic and aromatic metabolites. *Anal. Chem.* 2010; **82**: 4403–4412.
<https://doi.org/10.1021/ac100101d>.
- [23] Suto M, Kawashima H, Nakamura Y, Determination of Organic Acids in Honey by Liquid Chromatography with Tandem Mass Spectrometry. *Food Anal. Methods* 2020; **13**: 2249–2257. <https://doi.org/10.1007/s12161-020-01845-w>.
- [24] Moldoveanu SC, Poole T, Scott WA, An LC-MS method for the analysis of some organic acids in tobacco leaf, snus, and wet snuff. *Contrib. to Tob. Res.* 2018; **28**: 30–41.
<https://doi.org/10.2478/cttr-2018-0004>.
- [25] Berger TA, Demonstration of high speeds with low pressure drops using 1.8 μm particles in SFC. *Chromatographia* 2010; **72**: 597–602. <https://doi.org/10.1365/s10337-010-1699-2>.
- [26] Berger TA, Diffusion and Dispersion in Tubes in Supercritical Fluid Chromatography Using Sub-2 μm Packings. *Chromatographia* 2021; **84**: 167–177.
<https://doi.org/10.1007/s10337-020-03996-8>.
- [27] Haglind A, Hedeland M, Arvidsson T, Pettersson CE, Major signal suppression from

metal ion clusters in SFC/ESI-MS - Cause and effects. *J. Chromatogr. B* 2018; **1084**: 96–105. <https://doi.org/10.1016/j.jchromb.2018.03.024>.

- [28] Kruve A, Kaupmees K, Adduct Formation in ESI/MS by Mobile Phase Additives. *J. Am. Soc. Mass Spectrom.* 2017; **28**: 887–894. <https://doi.org/10.1007/s13361-017-1626-y>.
- [29] Ovchinnikov D V., Ul'yanovskii N V., Kosyakov DS, Pokrovskiy OI, Some aspects of additives effects on retention in supercritical fluid chromatography studied by linear free energy relationships method. *J. Chromatogr. A* 2022; **1665**: 462820. <https://doi.org/10.1016/j.chroma.2022.462820>.
- [30] Liigand J, Laaniste A, Kruve A, pH Effects on Electrospray Ionization Efficiency. *J. Am. Soc. Mass Spectrom.* 2017; **28**: 461–469. <https://doi.org/10.1007/s13361-016-1563-1>.
- [31] Cazenave-Gassiot A, Boughtflower R, Caldwell J, Hitzel L, Holyoak C, Lane S, Oakley P, Pullen F, Richardson S, Langley GJ, Effect of increasing concentration of ammonium acetate as an additive in supercritical fluid chromatography using CO₂-methanol mobile phase. *J. Chromatogr. A* 2009; **1216**: 6441–6450. <https://doi.org/10.1016/j.chroma.2009.07.022>.
- [32] Liigand J, de Vries R, Cuyckens F, Optimization of flow splitting and make-up flow conditions in liquid chromatography/electrospray ionization mass spectrometry. *Rapid Commun. Mass Spectrom.* 2019; **33**: 314–322. <https://doi.org/10.1002/rcm.8352>.
- [33] Akbal L, Hopfgartner G, Hyphenation of packed column supercritical fluid chromatography with mass spectrometry: where are we and what are the remaining challenges? *Anal. Bioanal. Chem.* 2020; **412**: 6667–6677. <https://doi.org/10.1007/s00216-020-02715-4>.
- [34] Pinkston JD, Advantages and drawbacks of popular supercritical fluid

chromatography/mass spectrometry interfacing approaches - A user's perspective. *Eur. J. Mass Spectrom.* 2005; **11**: 189–197. <https://doi.org/10.1255/ejms.731>.

- [35] Goetz GH, Farrell W, Shalaeva M, Sciabola S, Anderson D, Yan J, Philippe L, Shapiro MJ, High throughput method for the indirect detection of intramolecular hydrogen bonding. *J. Med. Chem.* 2014; **57**: 2920–2929. <https://doi.org/10.1021/jm401859b>.
- [36] West C, Lesellier E, Effects of mobile phase composition on retention and selectivity in achiral supercritical fluid chromatography. *J. Chromatogr. A* 2013; **1302**: 152–162. <https://doi.org/10.1016/j.chroma.2013.06.003>.
- [37] Gazárková T, Plachká K, Svec F, Nováková L, Current state of supercritical fluid chromatography-mass spectrometry. *TrAC - Trends Anal. Chem.* 2022; **149**: 116544. <https://doi.org/10.1016/j.trac.2022.116544>.
- [38] Mostafa ME, Grinias JP, Edwards JL, Supercritical Fluid Nanospray Mass Spectrometry. *J. Am. Soc. Mass Spectrom.* 2022; **33**: 1825–1832. <https://doi.org/10.1021/jasms.2c00134>.
- [39] Mostafa ME, Hayes MM, Grinias JP, Bythell BJ, Edwards JL, Supercritical Fluid Nanospray Mass Spectrometry: II. Effects on Ionization. *J. Am. Soc. Mass Spectrom.* 2023; In Press. <https://doi.org/10.1021/jasms.2c00372>.
- [40] Huang T, Armbruster M, Lee R, Hui DS, Edwards JL, Metabolomic analysis of mammalian cells and human tissue through one-pot two stage derivatizations using sheathless capillary electrophoresis-electrospray ionization-mass spectrometry. *J. Chromatogr. A* 2018; **1567**: 219–225. <https://doi.org/10.1016/j.chroma.2018.07.007>.

Figure Captions

Figure 1. Reaction scheme for derivatization of carboxylic acid groups with N-(4-aminophenyl)piperidine. Abbreviations: HATU - hexafluorophosphate azabenzotriazole tetramethyl uronium, DIPEA - N,N-diisopropylethylamine, DMF – dimethylformamide.

Figure 2. Extracted ion chromatograms of derivatized (red trace) and native (blue trace) lactic acid (A, both 3 ppm) and succinic acid (B, both 1 ppm). Both chromatograms were obtained using the HALO Penta-HILIC column (3 x 150 mm, 5 μ m particles) with a mobile phase composition (isocratic elution) of 85% CO₂:15% MeOH (with 10 mM ammonium acetate, pH 5.5) at 1.5 mL/min.

Figure 3. Calibration curves for the four derivatized (solid lines) and native (dashed lines) organic acids. Red circles are measured signals for lactate (A), blue squares are measured signals for succinate (B), black diamonds are measured signals for malate (C), and green triangles are measured signals for citrate (C). Error bars represent ± 1 S.D. from triplicate injections. Native forms of malate and citrate were not characterized, so only data for the derivatized compounds is shown in panel C.

Figure 4. Mass chromatograms (SIM mode) and mass spectra for derivatized succinate using 15% methanol with 10 mM ammonium acetate pH 5.5 (black trace for molecular ion SIM, relative intensities of three primary ion SIMs in B), no additive (red trace for molecular ion SIM, relative intensities of three primary ion SIMs in C), and 0.1% formic acid (blue trace for molecular ion SIM, relative intensities of three primary ion SIMs in D).

Figure 5. Mass chromatograms (SIM mode) at 435 m/z for derivatized succinate eluted using 15% methanol (w/ 10 mM ammonium acetate) modifier with no make-up flow (red trace), methanol make-up flow (black trace), and methanol (w/ 10 mM ammonium acetate) make-up flow (blue trace). Make-up flow rate was 0.15 mL/min when employed.

Figure 6. Separation comparison of derivatized organic acids using 15% methanol modifier (w/ 10 mM ammonium acetate, pH 5.5) for (A) HALO Penta-HILIC, (B) Phenomenex Luna Omega SUGAR, and (C) Phenomenex Chirex 3014. Compound concentrations for lactate (red trace), succinate (blue trace), malate (black trace), and citrate (green trace) were 200 ppb, 200 ppb, 1 ppm, and 10 ppm, respectively.

Figures

Figure 1.

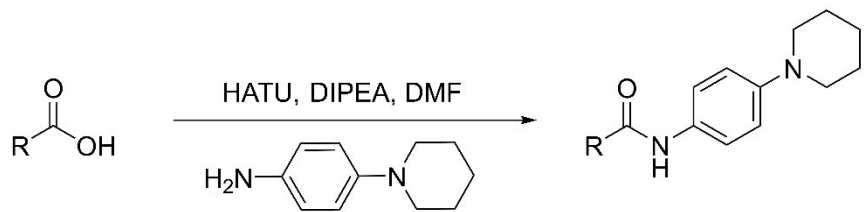


Figure 2.

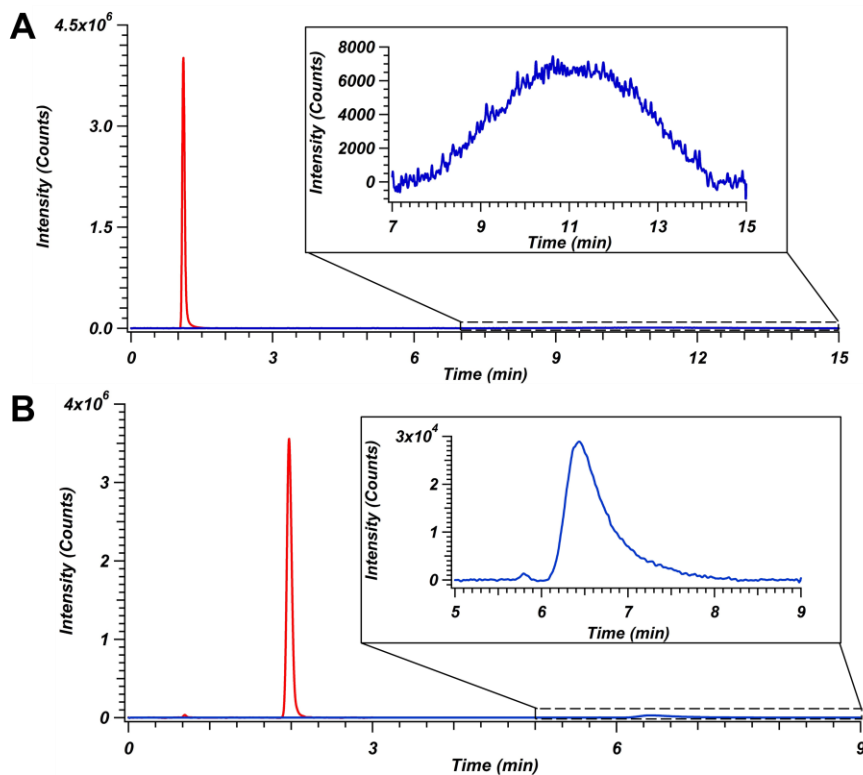


Figure 3.

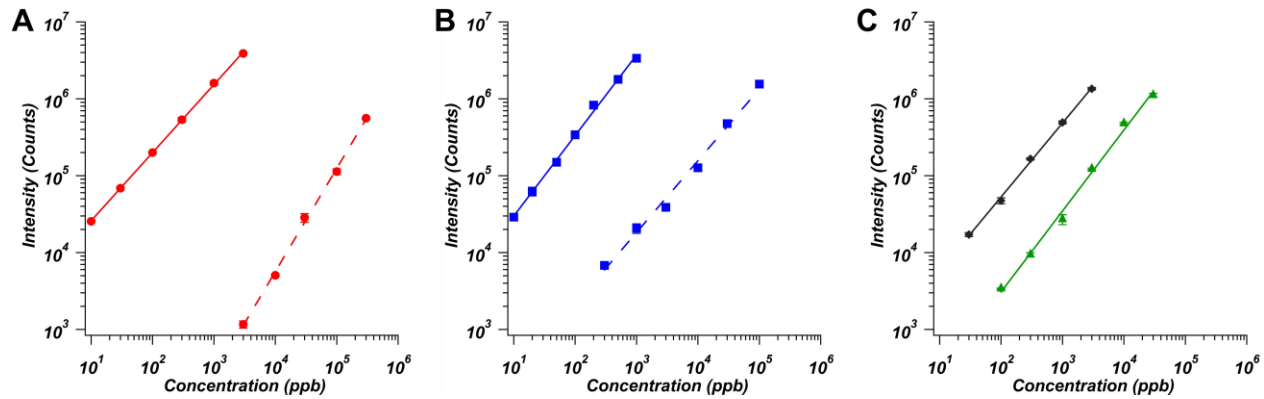


Figure 4.

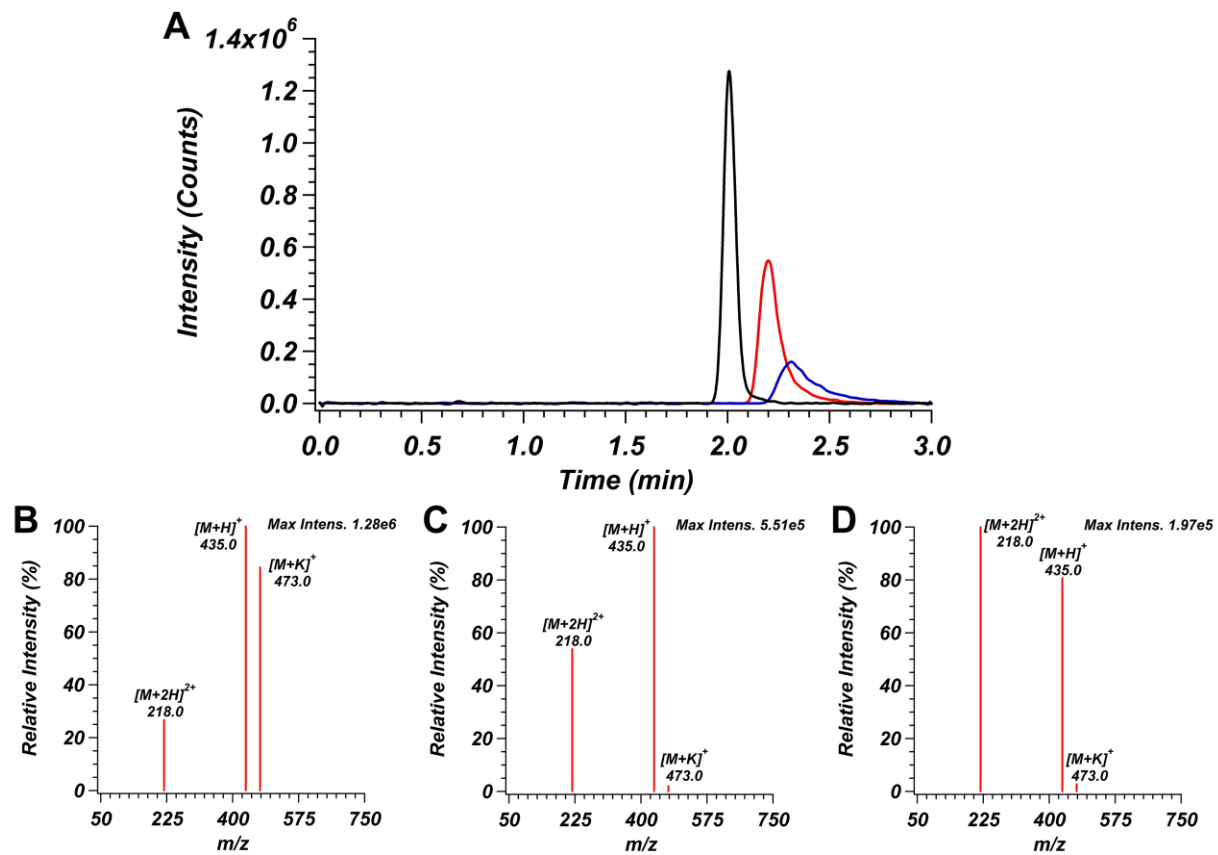


Figure 5.

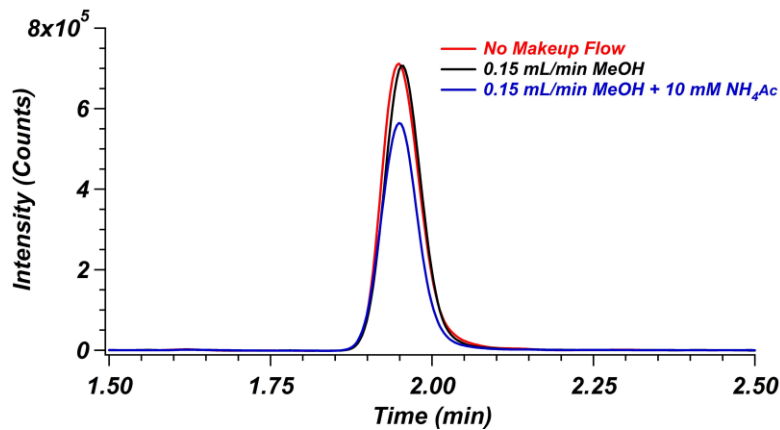
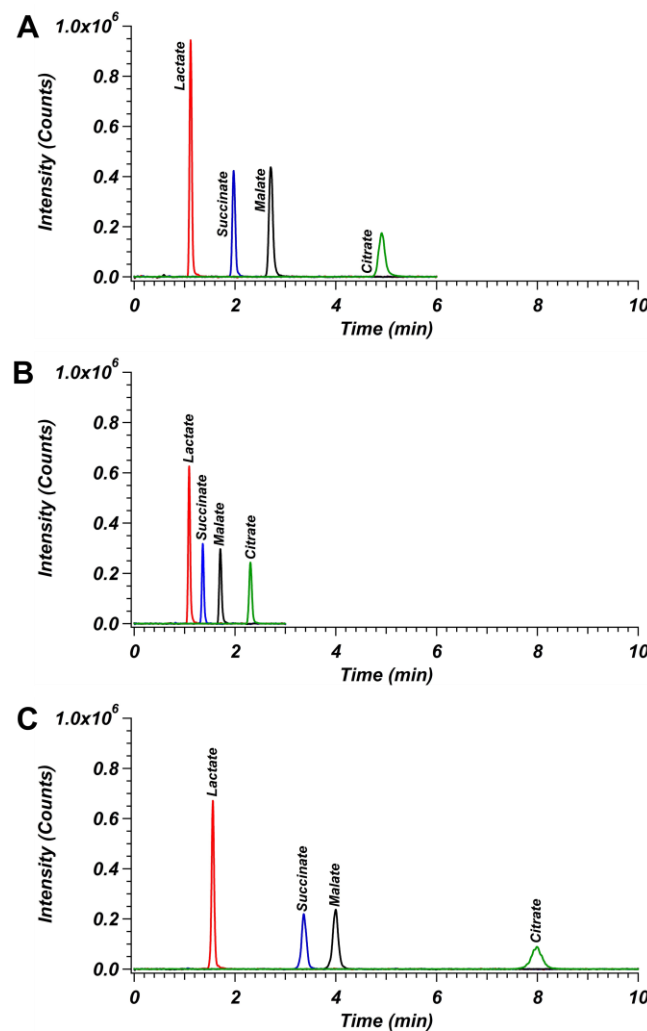


Figure 6.



Tables

Table 1. Figures of merit for native and derivatized organic acids (calculated using S/N ratio and peak height/intensity as described in the text). “N.D.” denotes “not detected”. Data were collected using the HALO Penta-HILIC column (3 x 150 mm, 5 μ m particles) with a mobile phase composition of 85% CO₂:15% MeOH (with 10 mM ammonium acetate, pH 5.5) at 1.5 mL/min. Error is listed as \pm 1 S.D. (triplicate analysis).

		<u>LOD</u> <u>(ppb)</u>	<u>LOQ</u> <u>(ppb)</u>	<u>Sensitivity</u> <u>(Counts/ppb)</u>
<i>Native Compounds</i>	Lactate	1070 \pm 60	3560 \pm 200	2.2 \pm 0.1
	Succinate	37 \pm 4	122 \pm 11	15.6 \pm 0.2
	Malate	N.D.	N.D.	N.D.
	Citrate	N.D.	N.D.	N.D.
<i>Derivatized Compounds</i>	Lactate	0.50 \pm 0.02	1.6 \pm 0.1	1290 \pm 50
	Succinate	1.5 \pm 0.3	5.1 \pm 1.1	3390 \pm 80
	Malate	2.6 \pm 0.4	8.7 \pm 1.3	450 \pm 10
	Citrate	8.5 \pm 1.3	28.4 \pm 4.4	38 \pm 2

**N-(4-aminophenyl)piperidine Derivatization to Improve Organic Acid Detection with
Supercritical Fluid Chromatography-Mass Spectrometry**

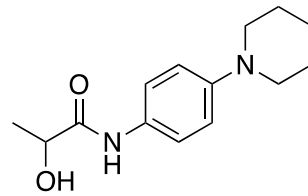
Supplementary Information

Synthesis and Characterization of Derivatized Organic Acids

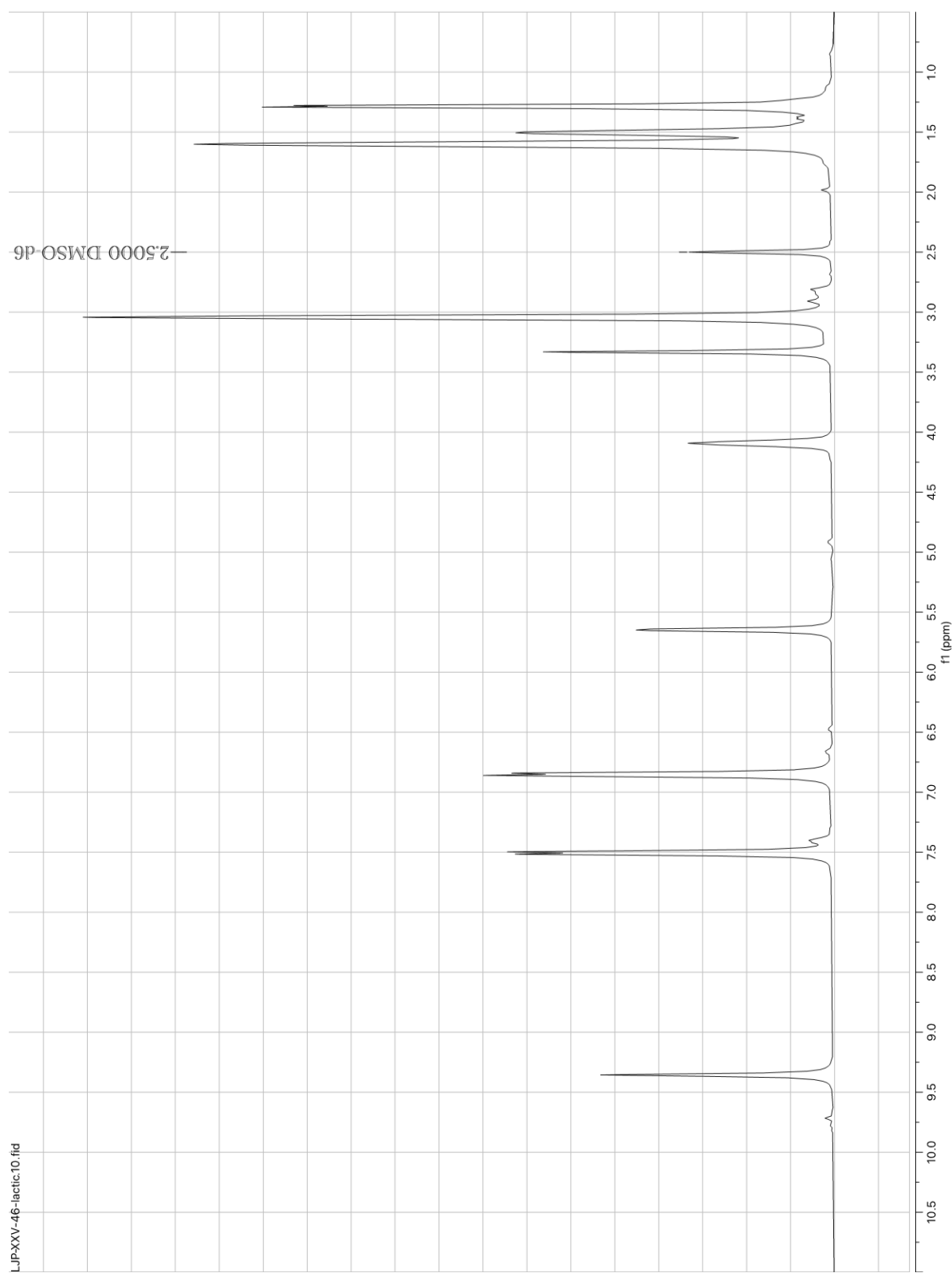
1. Lactic Acid

2-hydroxy-N-(4-(piperidin-1-yl)phenyl)propanamide.

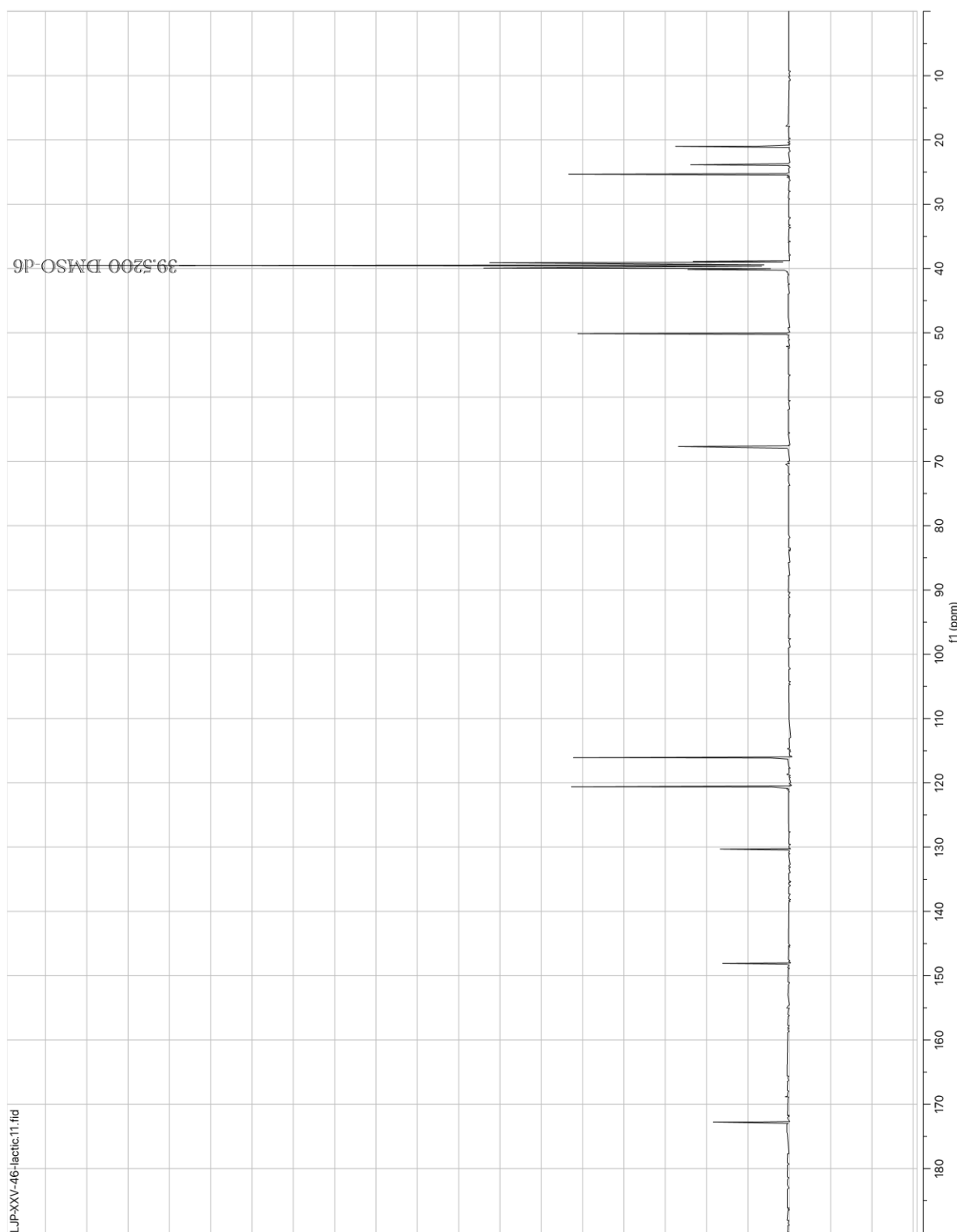
In a 20 mL vial equipped with a magnetic stir bar, lactic acid (12.4 μ L, 0.142 mmol, 1.0 eq) was dissolved in DMF (1.4 mL) and treated with DIPEA (74 μ L, 0.425 mmol, 3.0 eq.), N-(4-aminophenyl)piperidine (0.5 M in DMF, 283 μ L, 0.142 mmol, 1.0 eq) followed by HATU (64.7 mg, 0.170 mmol, 1.2 eq.). The resulting mixture was stirred at ambient temperature for 2 h, was poured into a separatory funnel containing 30 mL DCM and 30 mL saturated aqueous NaHCO₃. The layers were separated and the aqueous layer was extracted with DCM (2 x 20mL). The combined organic layers were washed with saturated aqueous NaCl solution, dried over Na₂SO₄, and concentrated *in vacuo*. The resulting crude mixture was purified by flash chromatography (Biotage Isolera, 60 μ m silica, 25 g column) using a gradient of 20% EtOAc/hexanes to 100% EtOAc to provide 2-hydroxy-N-(4-(piperidin-1-yl)phenyl)propanamide (32.5 mg, 0.131 mmol, 92%). ¹H-NMR (400MHz, DMSO-d6) δ 9.35 (s, 1H), 7.51 (d, *J*=7.3Hz, 2H), 6.84 (d, *J*=7.3Hz, 2H), 5.65 (s, 1H), 4.11-4.07 (m, 1H), 3.33-2.69 (m, 4H), 1.69-1.18 (m, 9H); ¹³C-NMR (101MHz, DMSO-d6) δ 172.8, 148.1, 130.3, 120.6, 116.1, 67.7, 50.1, 25.3, 23.9, 21.0. ESI-MS predicted for C₁₄H₂₁N₂O₂ 249.2 [M+H]⁺, observed 249.3.



¹H-NMR:



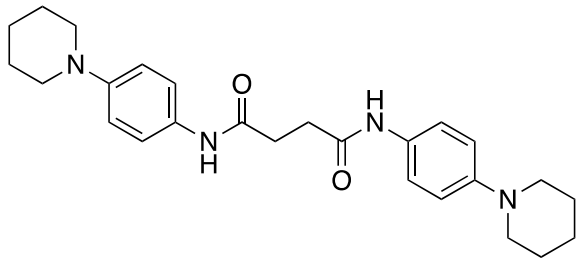
¹³C-NMR:



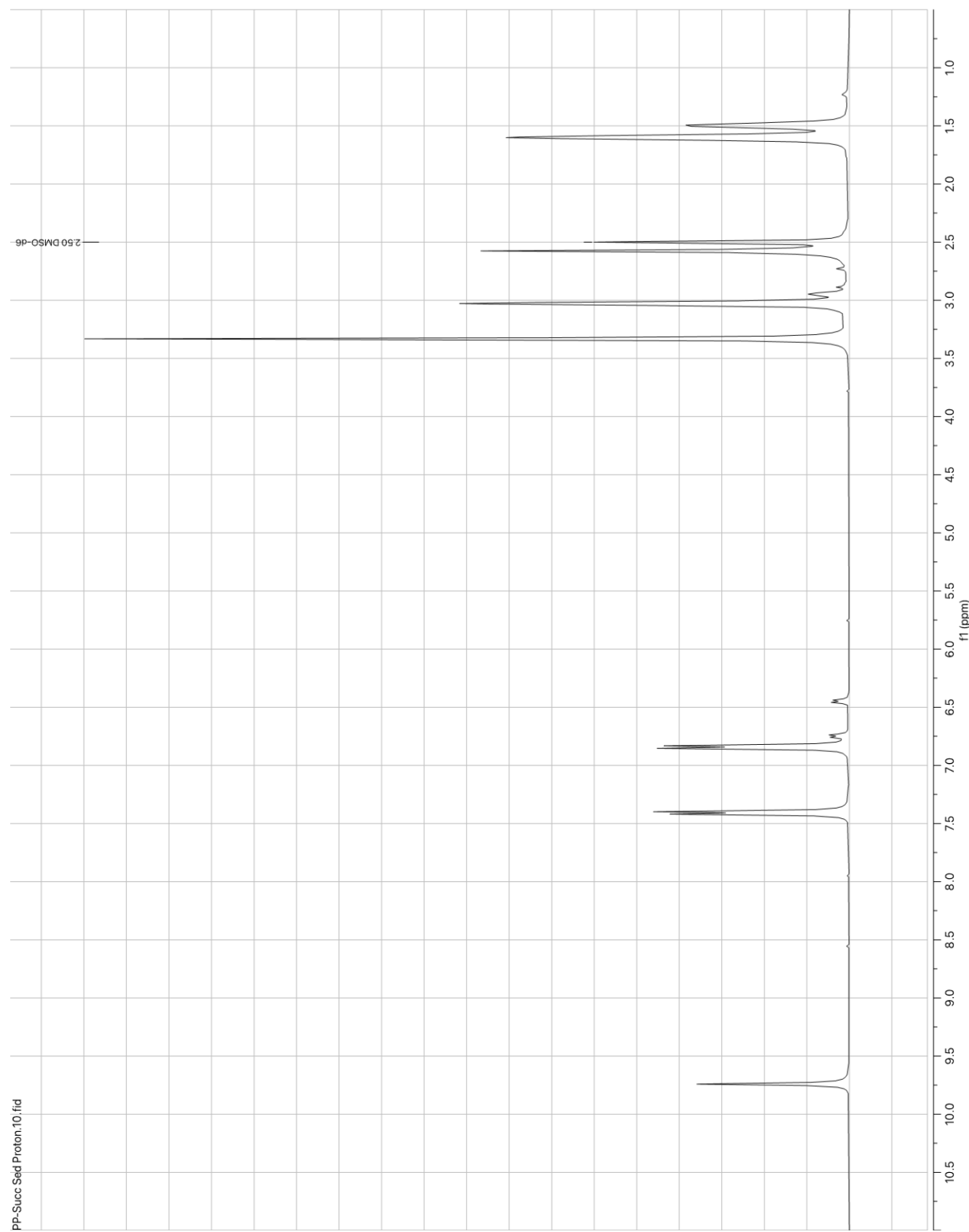
2. Succinic Acid

N¹,N⁴-bis(4-(piperidin-1-yl)phenyl)succinimide.

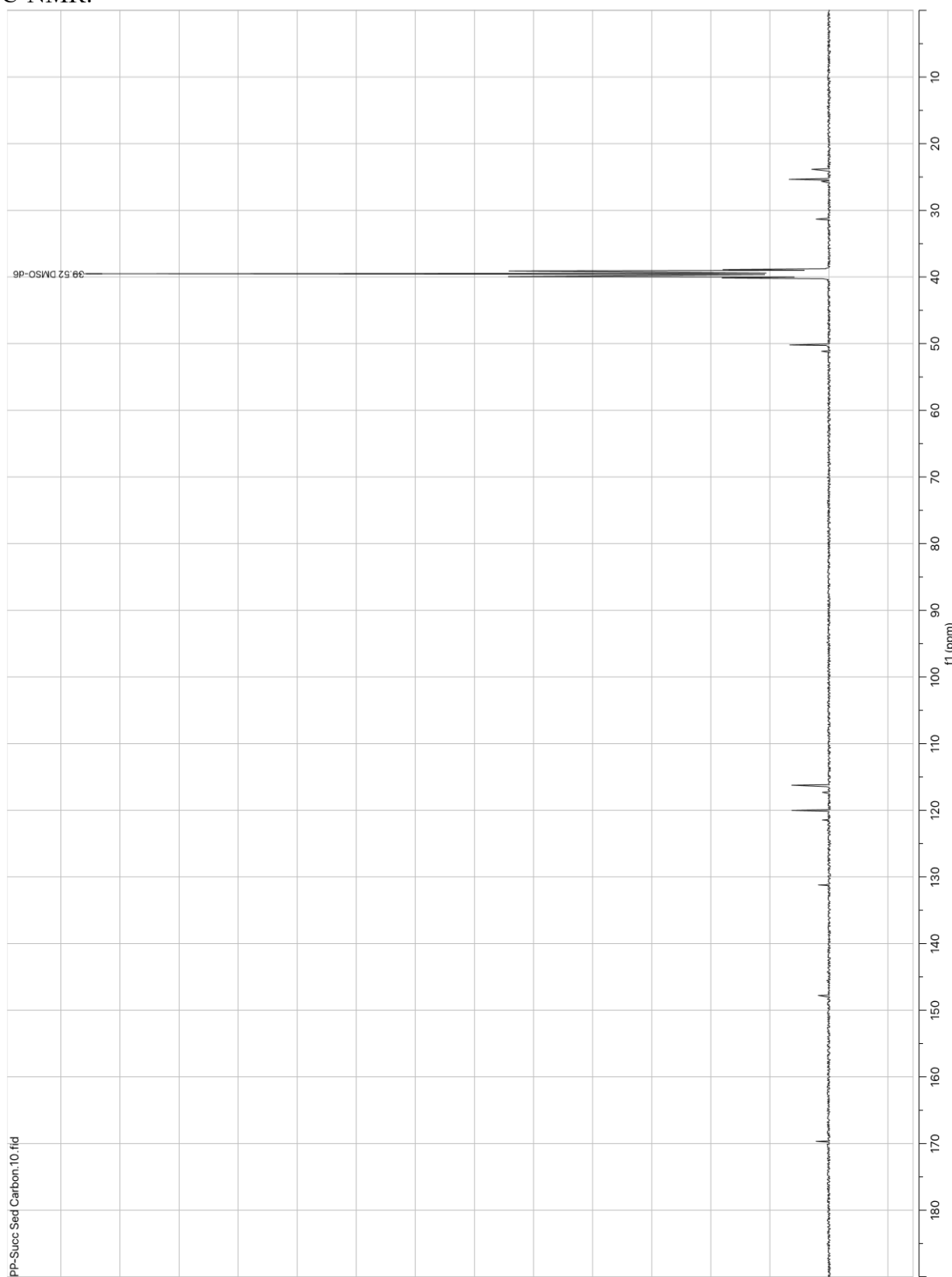
In a 20 mL vial equipped with a magnetic stir bar, sodium succinate (22.9 mg, 0.142 mmol, 1.0 eq) was dissolved in DMF (1.4 mL) and treated with DIPEA (74 μ L, 0.425 mmol, 3.0 eq.), N-(4-aminophenyl)piperidine (0.5 M in DMF, 566 μ L, 0.283 mmol, 2.0 eq) followed by HATU (129.4 mg, 0.340 mmol, 2.4 eq.). The resulting mixture was stirred at ambient temperature for 2 h, was poured into a separatory funnel containing 30 mL DCM and 30 mL saturated aqueous NaHCO₃. The layers were separated and the aqueous layer was extracted with DCM (2 x 20mL). The combined organic layers were washed with saturated aqueous NaCl solution, dried over Na₂SO₄, and concentrated *in vacuo*. The resulting crude mixture was purified by flash chromatography (Biotage Isolera, 60 μ m silica, 25 g column) using a gradient of 20% EtOAc/hexanes to 100% EtOAc to provide *N¹,N⁴-bis(4-(piperidin-1-yl)phenyl)succinimide* (43.8 mg, 0.101 mmol, 71%). ¹H-NMR (400MHz, DMSO-d6) δ 9.74 (s, 2H), 7.41 (d, *J* = 8.4Hz, 4H), 6.84 (d, *J* = 8.4Hz, 4H), 3.08-2.98 (m, 8H), 2.57 (s, 4H), 1.67-1.42 (m, 12H); ¹³C-NMR (101MHz, DMSO-d6) δ 169.7, 147.8, 131.2, 120.0, 116.3, 50.2, 31.3, 25.35, 23.9. ESI-MS predicted for C₂₆H₃₅N₄O₂ 435.3 [M+H]⁺, observed 435.3.



¹H-NMR:



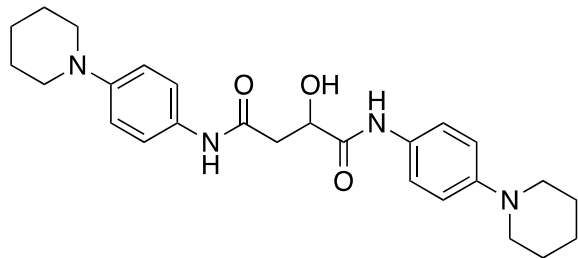
¹³C-NMR:



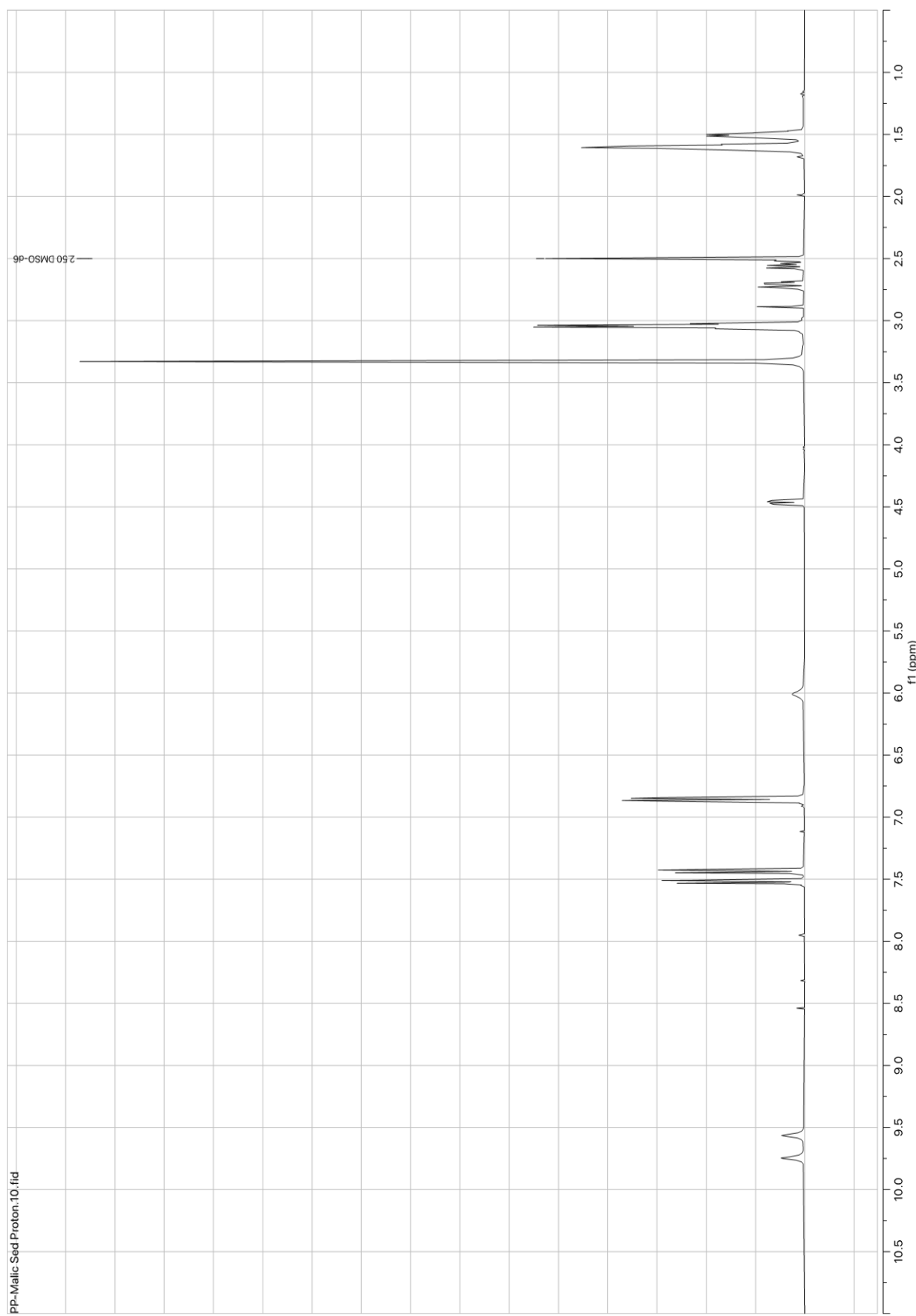
3. *Malic Acid*

2-hydroxy-*N*¹,*N*⁴-bis(4-(piperidin-1-yl)phenyl)succinimide.

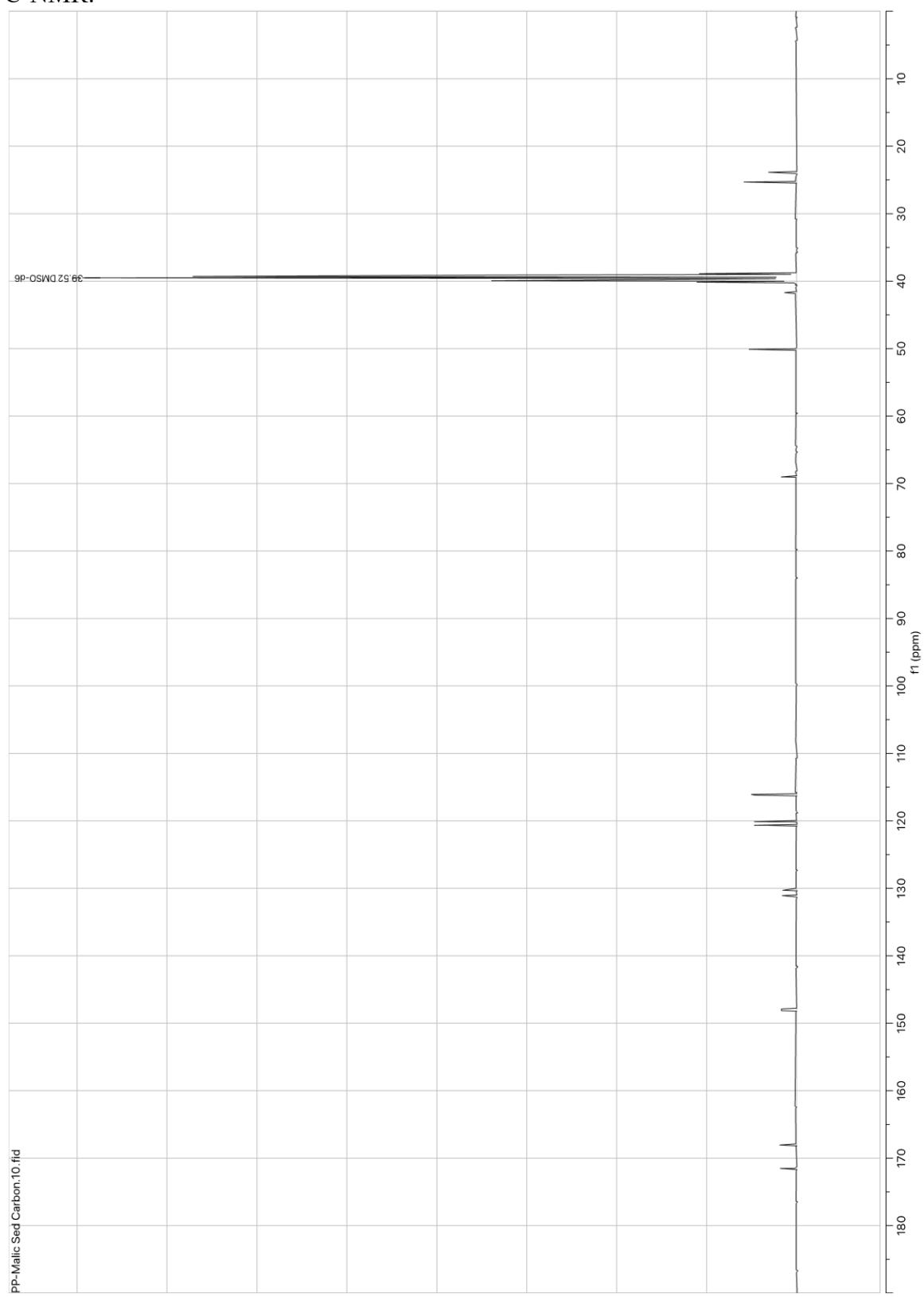
In a 20 mL vial equipped with a magnetic stir bar, malic acid (19.0 mg, 0.142 mmol, 1.0 eq) was dissolved in DMF (1.4 mL) and treated with DIPEA (74 μ L, 0.425 mmol, 3.0 eq.), N-(4-aminophenyl)piperidine (0.5 M in DMF, 566 μ L, 0.283 mmol, 2.0 eq) followed by HATU (129.4 mg, 0.340 mmol, 2.4 eq.). The resulting mixture was stirred at ambient temperature for 2h, was poured into a separatory funnel containing 30 mL DCM and 30 mL saturated aqueous NaHCO₃. The layers were separated and the aqueous layer was extracted with DCM (2 x 20mL). The combined organic layers were washed with saturated aqueous NaCl solution, dried over Na₂SO₄, and concentrated *in vacuo*. The resulting crude mixture was triturated with EtOAc and the insoluble pale brown solids were harvested to provide 2-hydroxy-*N*¹,*N*⁴-bis(4-(piperidin-1-yl)phenyl)succinimide (25.3 mg, 0.056 mmol, 40%). ¹H-NMR (400MHz, DMSO-d6) δ 9.76 (s, 1H), 9.56 (s, 1H), 7.52 (d, *J* = 8.3Hz, 2H), 7.44 (d, *J* = 9.1Hz, 2H), 6.85 (dd, *J* = 9.3, 2.1 Hz, 2H), 6.01 (s, 1H), 4.46 (dd, *J* = 8.9, 3.7 Hz, 1H), 3.08-3.01 (m, 8H), 2.75-2.67 (m, 1H), 2.60-2.51 (m, 1H), 1.67-1.54 (m, 8H), 1.54-1.45 (m, 4H); ¹³C-NMR (101MHz, DMSO-d6) δ 171.5, 168.1, 148.1, 147.9, 131.1, 130.3, 120.7, 120.1, 116.2, 116.1, 69.0, 50.2, 50.1, 41.7, 25.3, 25.3, 23.9. ESI-MS predicted for C₂₆H₃₅N₄O₃ 451.3 [M+H]⁺, observed 451.2.



¹H-NMR:



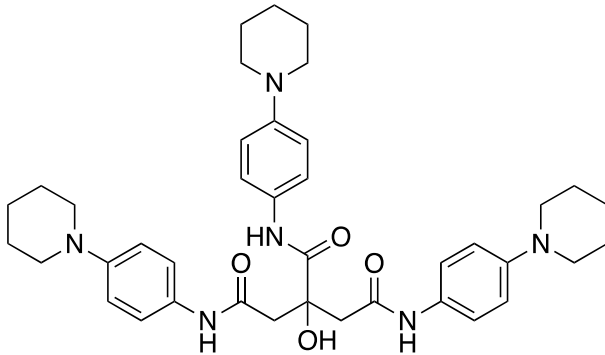
¹³C-NMR:



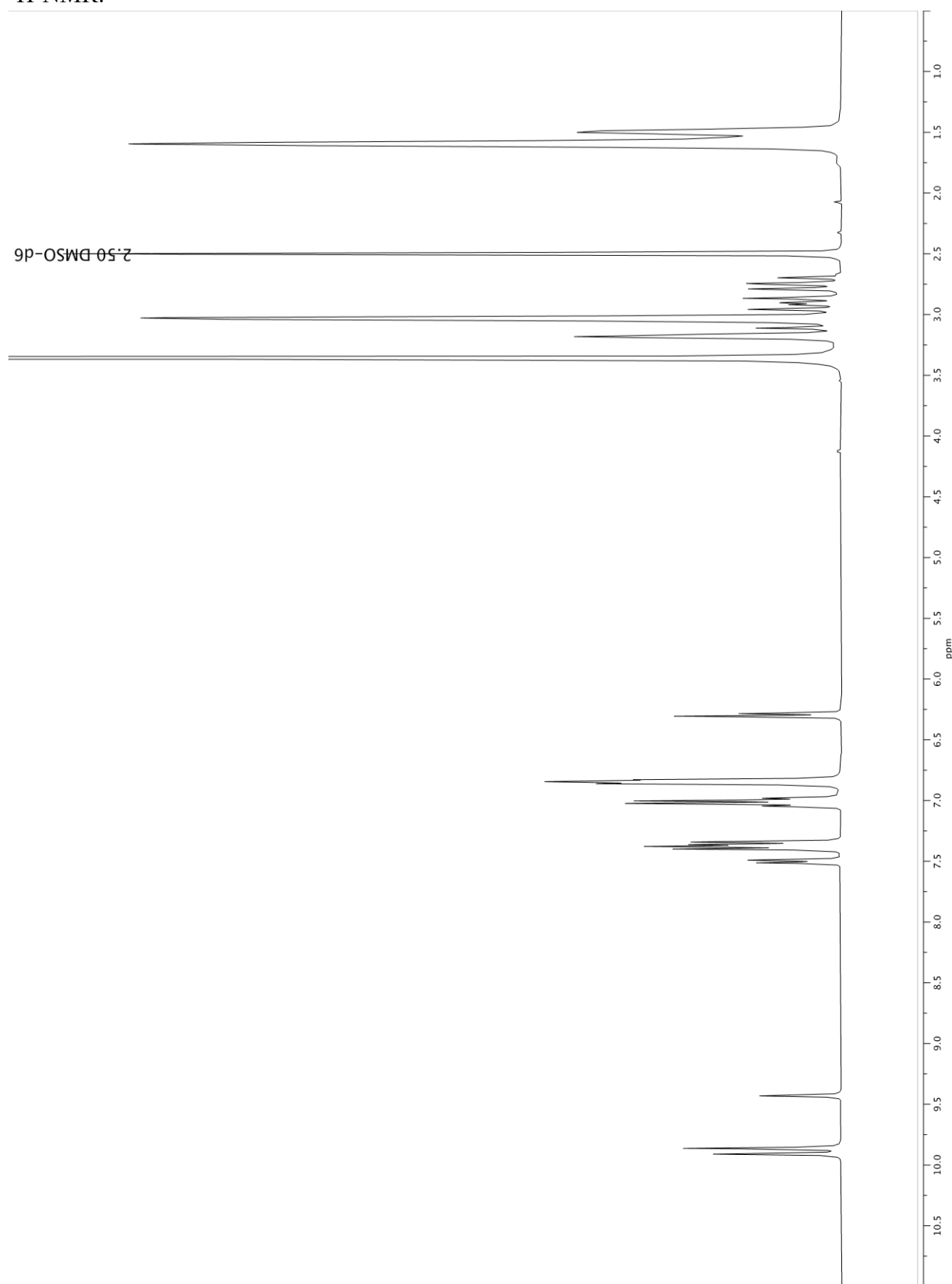
Citric Acid

2-hydroxy-*N*¹,*N*²,*N*³-tris(4-(piperidin-1-yl)phenyl)propane-1,2,3-tricarboxamide.

In a 20 mL vial equipped with a magnetic stir bar, malic acid (27.2 mg, 0.142 mmol, 1.0 eq) was dissolved in DMF (1.4 mL) and treated with DIPEA (222 μ L, 1.275 mmol, 9.0 eq.), N-(4-aminophenyl)piperidine (0.5 M in DMF, 852 μ L, 0.426 mmol, 3.0 eq) followed by HATU (194.1 mg, 0.510 mmol, 3.6 eq.). The resulting mixture was stirred at ambient temperature for 2 h, was poured into a separatory funnel containing 30 mL DCM and 30 mL saturated aqueous NaHCO₃. The layers were separated and the aqueous layer was extracted with DCM (2 x 20mL). The combined organic layers were washed with saturated aqueous NaCl solution, dried over Na₂SO₄, and concentrated *in vacuo*. The resulting crude mixture was triturated with EtOAc and the insoluble pale brown solids were harvested to provide 2-hydroxy-*N*¹,*N*²,*N*³-tris(4-(piperidin-1-yl)phenyl)propane-1,2,3-tricarboxamide (19.8 mg, 0.030 mmol, 21%). ¹H-NMR (400MHz, DMSO-d6) δ 9.91 (s, 1H), 9.86 (s, 1H), 9.43 (s, 1H), 7.50 (d, *J* = 9.1Hz, 1H), 7.41-7.32 (m, 3H), 7.06-6.96 (m, 3H), 6.89-6.79 (m, 3H), 6.29 (d, *J*=9.2Hz, 1H), 3.22-2.67 (m, 16H), 1.66-1.43 (m, 18H); ¹³C-NMR (101MHz, DMSO-d6) δ 178.5, 174.6, 172.1, 168.1, 167.2, 151.2, 148.1, 130.6, 130.4, 127.4, 122.7, 120.9, 116.2, 116.1, 115.4, 75.5, 72.2, 50.2, 50.1, 50.1, 49.3, 25.4, 25.1, 23.9. ESI-MS predicted for C₃₉H₅₁N₆O₄ 667.4 [M+H]⁺, observed 667.5.



¹H-NMR:



¹³C-NMR:

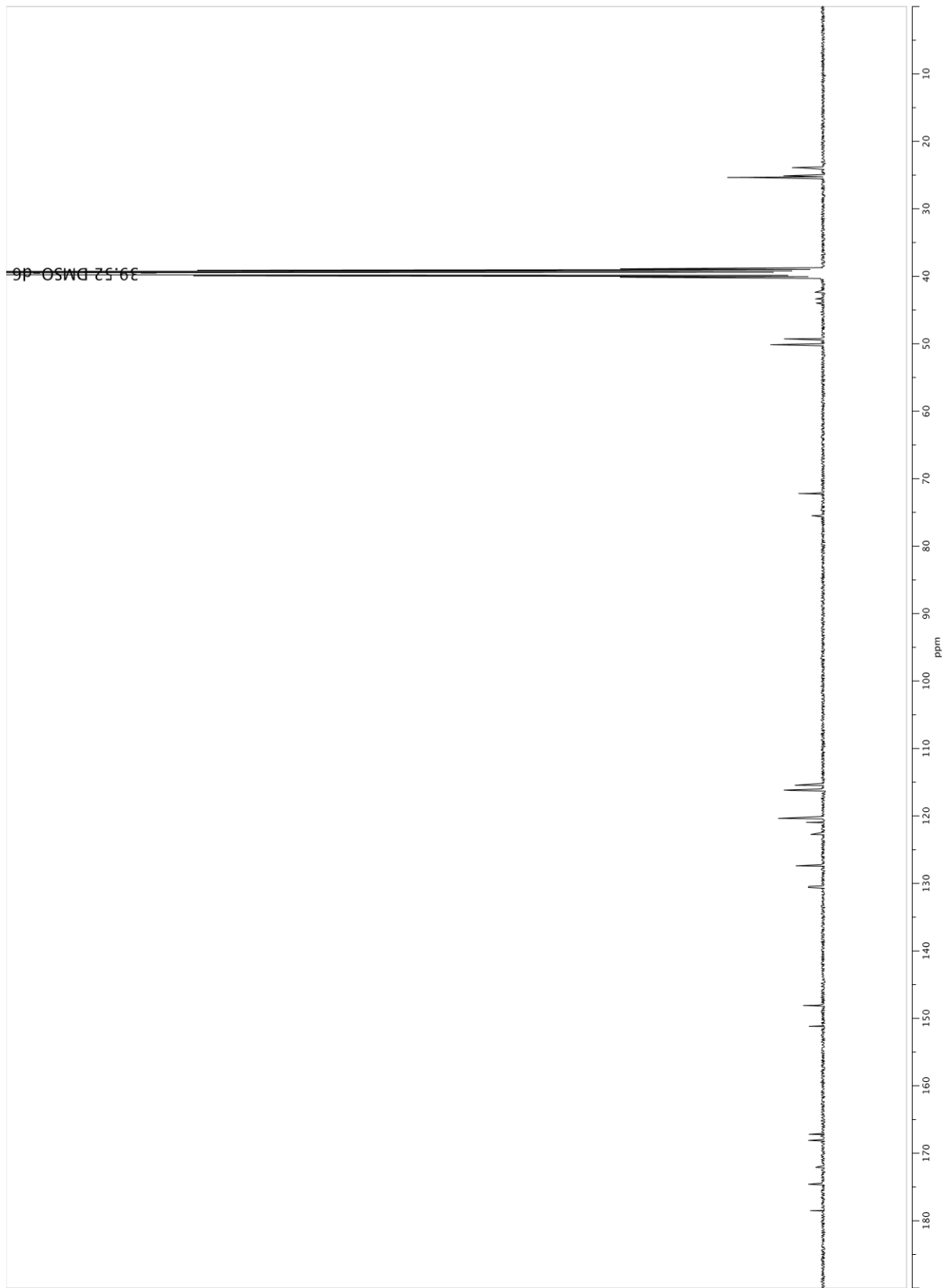


Table S1. MS parameters used for full scan detection of native and derivatized organic acids.

	<u>Native Compounds</u>	<u>Derivatized Compounds</u>
<i>Scan Range (m/z)</i>	50-200	50-750
<i>Ionization Mode</i>	(-)	(+)
<i>Interface Temperature (°C)</i>	350	350
<i>Desolvation Line Temperature (°C)</i>	250	250
<i>Heat Block Temperature (°C)</i>	200	200
<i>Nebulizing Gas Flow (L/min)</i>	1.5	1.5
<i>Interface Voltage (kV)</i>	-3.6	3.6
<i>Desolvation Line Voltage (V)</i>	-20	0
<i>Q_{array} DC (V)</i>	-10	0
<i>Q_{array} RF (V)</i>	26	39

Table S2. Measured mass-to-charge ratios (m/z) of the native and derivatized organic acids of interest, with bold m/z values corresponding to ion used for calibration curve analysis by SIM.

<u>Compound</u>	<u>Molar Mass</u> <u>(g/mol)</u>	<u>Native</u> <u>Compounds</u> <u>(m/z)</u>	<u>Derivatized</u> <u>compounds</u> <u>(m/z)</u>
<i>Lactate</i>	90.08	89 [M-H] ⁻	249 [M+H] ⁺
<i>Succinate</i>	118.09	117 [M-H] ⁻	435 [M+H] ⁺ 218 [M+2H] ²⁺
<i>Malate</i>	134.09	133 [M-H] ⁻	451 [M+H] ⁺ 226 [M+2H] ²⁺
<i>Citrate</i>	192.12	191 [M-H] ⁻	667 [M+H] ⁺ 334 [M+2H] ²⁺ 223 [M+3H] ³⁺

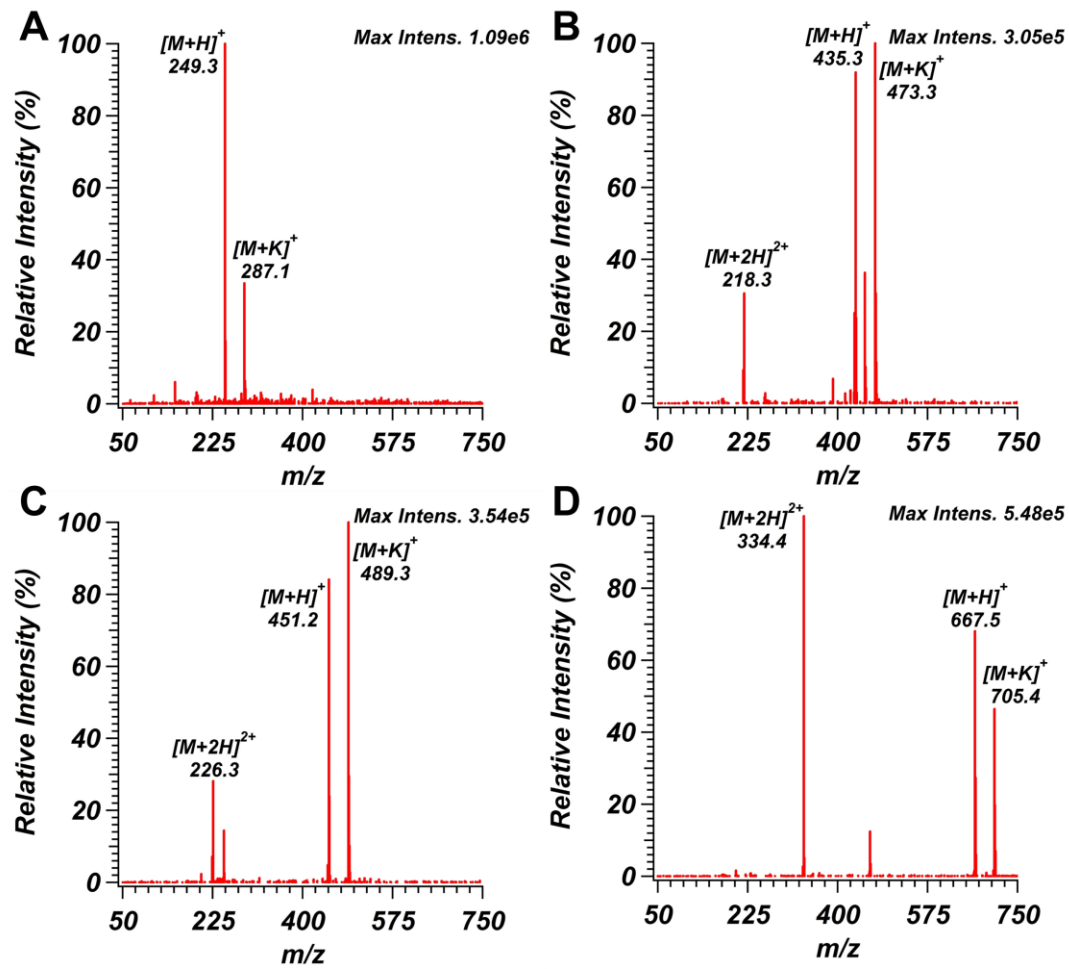


Figure S1. Peak mass spectra from Penta-HILIC separation for derivatized (A) lactate, (B) succinate, (C) malate, and (D) citrate.

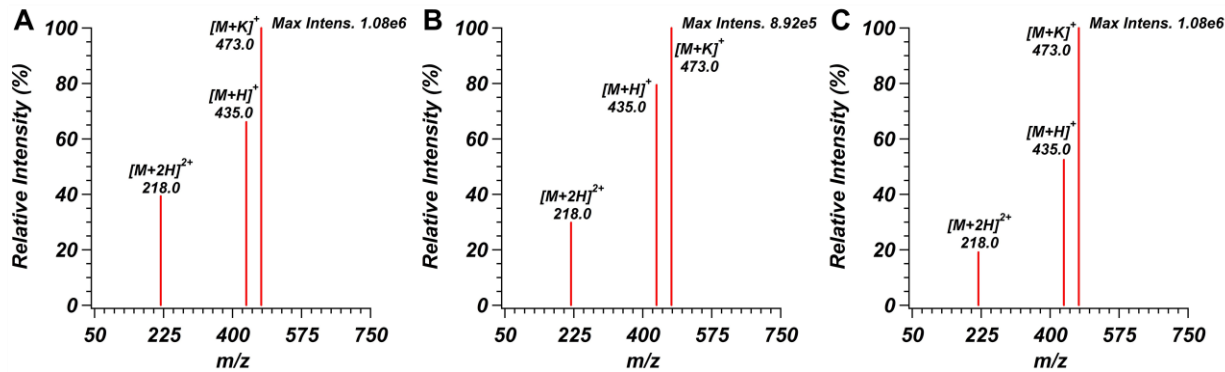


Figure S2. Mass spectra of derivatized succinate using no make-up flow (A), methanol as a make-up flow solvent (B), and methanol (w/ 10 mM ammonium acetate) as a make-up flow solvent (C).

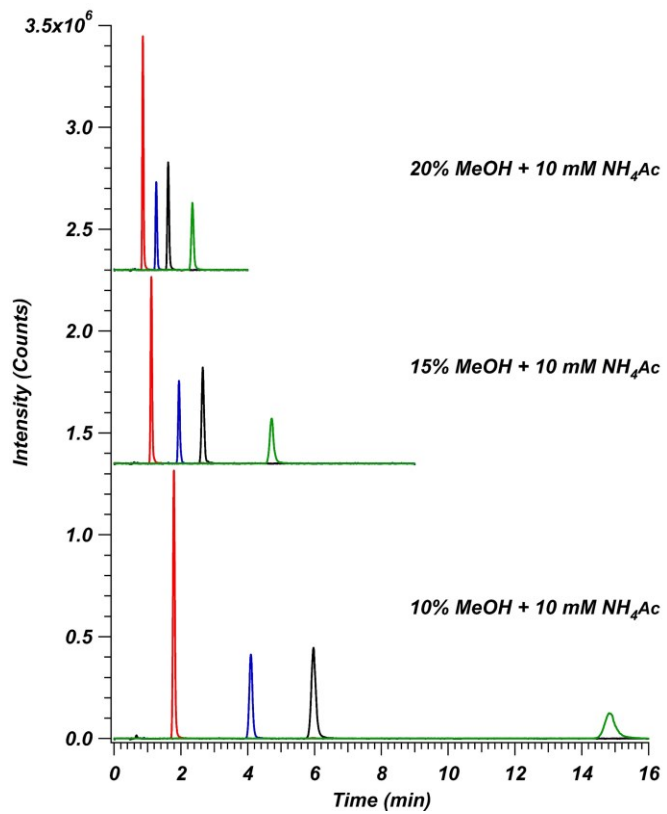


Figure S3. Separation of four derivatized organic acids (lactate (red trace), succinate (blue trace), malate (black trace), and citrate (green trace)) on the Penta-HILIC column at (A) 10%, (B) 15%, and (C) 20% methanol modifier (all w/ 10 mM ammonium acetate, pH 5.5).

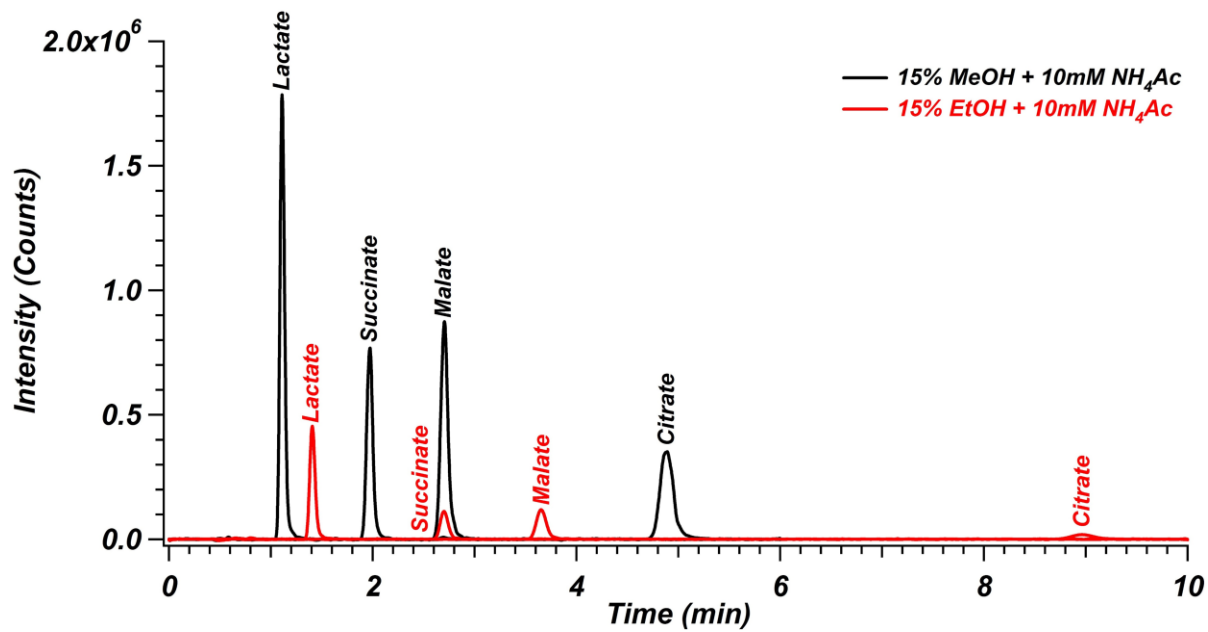


Figure S4. Separation of derivatized organic acids on the Penta-HILIC column using methanol (w/ 10 mM ammonium acetate, pH 5.5) (black trace) and ethanol (w/ 10mM ammonium acetate, pH 5.5) (red trace), both at 15% modifier concentration.